Journal of Theoretical and Applied Information Technology
20th January 2013. Vol. 47 No.2

ISSN: 1992-8645 www.jatit.org E-ISSN: 1817-3195

SMALL SIGNAL ANALYSIS OF FLEXIBLE AC TRANSMISSION SYSTEM USING INTERLINE POWER FLOW CONTROLLER (IPFC)

[1]CH. VENKATA KRISHNA REDDY, [2] K.KRISHNA VENI, [3]G.TULASIRAM DAS, [4]SIRAJ

[1]Asst. Prof., Department of EEE, CBIT, Gandipet, Hyderabad, India
[2] Prof., Department of EEE, CBIT, Gandipet, Hyderabad, India
[3] Prof., Department of EEE, JNTUH, Hyderabad, India
[4] ME, Department of EEE, CBIT, Hyderabad, India

E-mail: c_h_v_k_r@yahoo.com

ABSTRAC

The Interline Power Flow Controller (IPFC) is a voltage-source-converter (VSC)-based flexible ac transmission system (FACTS) controller which can inject a voltage with controllable magnitude and phase angle at the line-frequency thereby providing compensation among multiple transmission lines. In this paper, the use of the IPFC based controller in damping of low frequency oscillations is investigated. An extended Heffron-Phillips model of a single machine infinite bus (SMIB) system installed with IPFC is established and used to analyze the damping torque contribution of the IPFC damping control to the power system. The potential of various IPFC control signals upon the power system oscillation stability is investigated a using controllability index. The effect of this damping controller on the system, subjected to wide variations in loading conditions and system parameters, is investigated. Results of simulation investigations in Matlab are presented to validate the proposed approach.

Key words — *FACTS, IPFC, Damping, Small Signal Stability*

NOTATIONS:

P_A : transferred power of primary line,

P_B : transferred power of secondary line,

P_e : Total transferred power of lines,

V_s : Terminal voltage of generator,

I_{id} : Direct axis current of line i,

C : dc link capacitance

H : inertia constant (M = 2H)

m_i : Modulation index of series converter

δ_i : Phase angle of series converter voltage

V_b : Infinite bus voltage

V_{dc} : Voltage at dc link

V_t : Terminal voltage of the generator

X'_d : Direct axis transient synchronous reactance of generator

K_A : AVR Gain

T_A : Time constant of AVR

I_{iq} : Quadrature axis current of line i,

X_d : Direct axis steady-state synchronous reactance of generator

X_q : Quadrature axis steady-state synchronous reactance of generator,

X_t : Reactance of series coupling transformer,

Journal of Theoretical and Applied Information Technology
20th January 2013. Vol. 47 No.2

ISSN: 1992-8645 www.jatit.org E-ISSN: 1817-3195

1. INTRODUCTION

Low frequency oscillations with frequency in the range of 0.2 to 2.0 Hz are one of the results of the interconnection of large power systems. Modem power systems are stable if electromechanical oscillations occurring in each area can be damped as soon as possible. To increase power system oscillations stability, Power System Stabilizer (PSS) is a simple, effective, and economical method [1].

"Flexible AC Transmission Systems (FACTS)" technology has been proposed during the last three decades and provides better utilization of existing systems. Interesting FACTS capabilities such as power flow control, damping of power system oscillations, voltage regulation, and reactive power compensation make them a good option for effective utilization of power systems. In this paper one of the FACTS capabilities is damping inter-area oscillations that will be accurately investigated for IPFC.

Interline Power Flow Controller, which is proposed by Guygyi and etal [2] in l998, is a FACTS controller for series compensation with unique capability of power flow management between multi-lines of a substation. In the IPFC structure a number of inverters are linked together at their dc terminals. Each inverter can provide series reactive compensation, as an SSSC, for its own line. However, the inverters can transfer real power between them via their common dc terminal. This capability allows the IPFC to provide both reactive and real compensation for some of the lines and thereby optimize the utilization of the overall transmission system.

Like other FACTS elements, IPFC can be used for increasing power system stability against large and small disturbances.

In this paper the voltage of coupling capacitance between two VSC-based converters is used as a state variable. Output power of the generator is used as an input of PI controller, which creates proper amplitude modulation ratio for the secondary converter.

2. DYNAMIC MODEL OF THE SYSTEM WITH IPFC

A single-machine infinite-bus (SMIB) system with IPFC, installed on two lines is considered. This configuration which consists of two parallel transmission lines, connects the generator G to an infinite bus, is illustrated in figure 1.

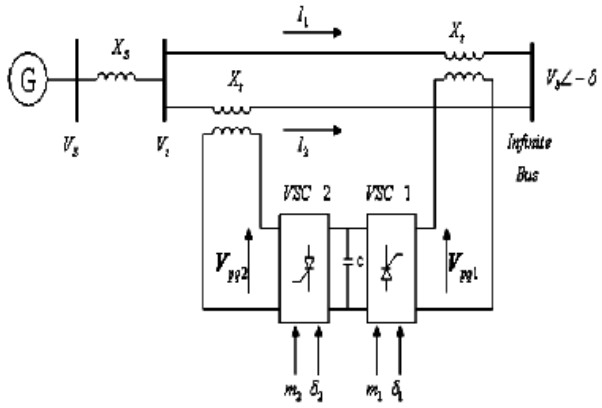

Figure 1 Single Machine Infinite Bus System With IPFC

PSS is not taking into account in the power system. Operating conditions and parameters are represented in the appendix.

Phillips-Heffron linear model of a single-machine infinite bus system with IPFC is derived from the nonlinear differential equations. Neglecting the resistances of all the components of the system like generators, transformers, transmission lines, and series converter transformers, a nonlinear dynamic model of the system is derived as follows:

$$\dot{\delta} = \omega_{\circ}(\omega - 1) \quad \text{-------- (1)}$$

$$\dot{\omega} = \frac{[P_m - P_e - D(\omega - 1)]}{M} \quad \text{--------- (2)}$$

$$\dot{E}'_q = \left(-E_q + E'_{fd}\right)/T'_{do} \quad \text{--------- (3)}$$

$$\dot{E}_{fd} = \left[-E_{fd} + K_A\left(V_{ref} - V_s\right)\right]/T_A \quad \text{---------(4)}$$

Where,

$$P_e = P_1 + P_2 \quad \text{-------- (5)}$$

$$P_e = V_{sd}(I_{1d} + V_{sq} I_{2d}) + (I_{1q} + I_{2q}) \quad \text{--------- (6)}$$

$$E_q = E'_q + (X_d - X'_d)(I_{1d} + I_{2d}) \quad \text{------- (7)}$$

$$V_s = V_{sd} + \mathrm{j} V_{sq} \quad \text{--------- (8)}$$

$$= X_q I_{1q} + \mathrm{j}[E'_q - X'_d (I_{1d} + I_{2d})]$$

Journal of Theoretical and Applied Information Technology
20th January 2013. Vol. 47 No.2

ISSN: 1992-8645 www.jatit.org E-ISSN: 1817-3195

If the general Pulse Width Modulation (PWM) is used for VSCs, the voltage equations of the IPFC converters in dq coordinates will be [1]:

$$\begin{bmatrix} V_{p1} \\ V_{q1} \end{bmatrix} = \begin{bmatrix} 0 & -X_t \\ X_t & 0 \end{bmatrix} \begin{bmatrix} I_{1d} \\ I_{1q} \end{bmatrix} + \frac{V_{dc}}{2} \begin{bmatrix} m_1 \cos\delta_1 \\ m_2 \cos\delta_2 \end{bmatrix} \quad \text{-------- (9)}$$

$$\begin{bmatrix} V_{p2} \\ V_{q2} \end{bmatrix} = \begin{bmatrix} 0 & -X_t \\ X_t & 0 \end{bmatrix} \begin{bmatrix} I_{2d} \\ I_{2q} \end{bmatrix} + \frac{V_{dc}}{2} \begin{bmatrix} m_1 \sin\delta_1 \\ m_2 \sin\delta_2 \end{bmatrix} \quad \text{-------- (10)}$$

where,

$$V_{pqK} = V_{pK} + \mathbf{j} V_{qK} = V_{pqK}\, e^{j\delta_k} \quad \text{---------- (11)}$$

$$\frac{dV_{dc}}{dt} = \frac{3m_1}{4C}\left[I_{1d}\cos\delta_1 + I_{1q}\sin\delta_1\right] + \frac{3m_2}{4C}\left[I_{2d}\cos\delta_2 + I_{2q}\sin\delta_2\right] \quad \text{---------- (12)}$$

From figure 1, we have:

$$V_s = \mathrm{j}\, X_s\, I_s + V_{pq2} + \mathrm{j}\, X_L\, I_2 \quad \text{--------- (13)}$$

This equation in d-q coordinates is as follows:

$$V_{sd} + \mathrm{j} V_{sq} = \mathrm{j}\, X_s [(I_{1d} + I_{2d}) + \mathrm{j}(I_{1q} + I_{2q})] + \mathrm{j}\, X_L (I_{2d} + \mathrm{j}\, I_{2q}) + V_{p2} + V_b \sin\delta + jV_b \cos\delta \quad \text{---------- (14)}$$

In the other hand, according to figure 2, we have:

$$V_{sd} = X_q (I_{1q} + I_{2q}) \quad \text{---------- (15)}$$

$$V_{sq} = E'_q - (X_d - X'_d)(I_{1d} + I_{2d}) \quad \text{--------- (16)}$$

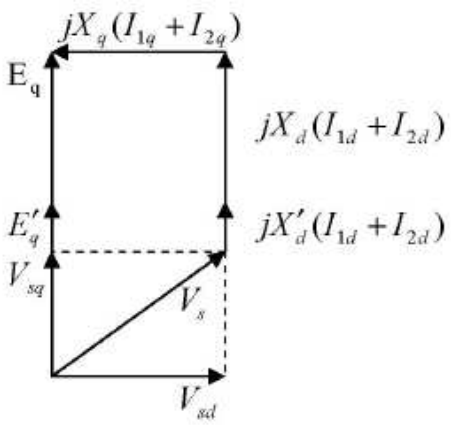

Figure 2.Phasor diagram of investigated system

From (6) to (12), it can be obtained:

$$\begin{bmatrix} X_{ds} & X_{d\Sigma} \\ X_{TL} & -X_{TL} \end{bmatrix} \begin{bmatrix} I_{1d} \\ I_{2d} \end{bmatrix} = \begin{bmatrix} E'_q - \frac{V_{dc}}{2} m_2 \sin\delta_2 - V_b \cos\delta \\ \frac{V_{dc}}{2}(m_2 \sin\delta_2 - m_1 \sin\delta_1) \end{bmatrix} \quad \text{----- (17)}$$

$$\begin{bmatrix} X_{qs} & X_{q\Sigma} \\ -X_{TL} & X_{TL} \end{bmatrix} \begin{bmatrix} I_{1q} \\ I_{2q} \end{bmatrix} = \begin{bmatrix} \frac{V_{dc}}{2} m_2 \cos\delta_2 + V_b \sin\delta \\ \frac{V_{dc}}{2}(m_2 \cos\delta_2 - m_1 \cos\delta_1) \end{bmatrix} \quad \text{----- (18)}$$

where,

$$X_{qs} = X_q + X_s \quad \text{-------- (19)}$$

$$X_{TL} = X_t + X_L \quad \text{-------- (20)}$$

$$X_{dK} = X_{ds} - X_{TL} \quad \text{-------- (21)}$$

$$X_{qK} = X_{qs} + X_{TL} \quad \text{-------- (22)}$$

$$X_{ds} = X'_d + X_s \quad \text{-------- (23)}$$

and X_L is the series reactance of each transmission line.

3. LINEAR DYNAMIC MODEL

Power system oscillation stability and control can be studied using a linearized model of the power systems.

A linear dynamic model of the system illustrated in figurel, is obtained by linearising the nonlinear model of the system presented in above section,

Journal of Theoretical and Applied Information Technology
20th January 2013. Vol. 47 No.2

ISSN: 1992-8645 www.jatit.org E-ISSN: 1817-3195

around an operating condition. The linearized model is as follows:

$$\begin{bmatrix} \Delta\dot{\delta} \\ \Delta\dot{\omega} \\ \Delta\dot{E}_q^1 \\ \Delta\dot{E}_{fd} \\ \Delta\dot{V}_{dc} \end{bmatrix} = \begin{bmatrix} 0 & \omega_o & 0 & 0 & 0 \\ \frac{-K_1}{M} & \frac{-D}{M} & \frac{-K_2}{M} & 0 & -\frac{K_{pv}}{M} \\ \frac{-K_4}{T'_{do}} & 0 & \frac{-K_3}{T'_{do}} & \frac{1}{T'_{do}} & \frac{-K_{qv}}{T'_{do}} \\ \frac{-K_A K_5}{T_A} & 0 & -\frac{K_A K_6}{T_A} & \frac{1}{T_A} & -\frac{K_A K_{vv}}{T_A} \\ K_7 & 0 & K_8 & 0 & -K_9 \end{bmatrix} \begin{bmatrix} \Delta\delta \\ \Delta\omega \\ \Delta E_q^1 \\ \Delta E_{fd} \\ \Delta V_{dc} \end{bmatrix} +$$

$$+ \begin{bmatrix} 0 & 0 & 0 & 0 \\ -\frac{K_{pm1}}{M} & -\frac{K_{p\delta 1}}{M} & -\frac{K_{pm2}}{M} & -\frac{K_{p\delta 2}}{M} \\ \frac{-K_{qm1}}{T'_{do}} & \frac{-K_{q\delta 1}}{T'_{do}} & \frac{-K_{qm2}}{T'_{do}} & \frac{-K_{q\delta 2}}{T'_{do}} \\ -\frac{K_A K_{vm1}}{T_A} & -\frac{K_A K_{v\delta 1}}{T_A} & -\frac{K_A K_{vm2}}{T_A} & -\frac{K_A K_{v\delta 2}}{T_A} \\ K_{cm1} & K_{c\delta 1} & K_{cm2} & K_{c\delta 2} \end{bmatrix} \begin{bmatrix} \Delta m_1 \\ \Delta\delta_1 \\ \Delta m_2 \\ \Delta\delta_2 \end{bmatrix}$$

-------- (24)

In the state-space representation, the power system can be modeled as

$$\dot{X} = AX + BU$$

Where the state vector and control vector are as follows:

$$X = \begin{bmatrix} \Delta\delta & \Delta\omega & \Delta E_q^{'} & \Delta E_{fd} & \Delta V_{dc} \end{bmatrix}^T$$

$$U = \begin{bmatrix} \Delta m_1 & \Delta\delta_1 & \Delta m_2 & \Delta\delta_2 \end{bmatrix}^T$$

Δm_1 is the deviation in pulse width modulation index m_1 of voltage series converter-1 in line-1. By controlling m_1, the magnitude of series injected voltage in line-1 can be controlled.

Δm_2 is the deviation in pulse width modulation index m_2 of voltage series converter-2 in line-2.By controlling m_2, the magnitude of series injected voltage in line-2 can be controlled.

$\Delta\delta_1$ is the deviation in phase angle of the injected voltage V_{pq1}.

$\Delta\delta_2$ is the deviation in phase angle of the injected voltage V_{pq2}.

ΔV_{dc} is the deviation of coupling capacitance voltage between converters,

Using the mathematical model of the SMIB with IPFC as state space representation in (24), the Phillips-Heffron model or linear model of the SMIB system can be obtained including IPFC [3].

Where

$$U = \begin{bmatrix} \Delta m_1 & \Delta\delta_1 & \Delta m_2 & \Delta\delta_2 \end{bmatrix}^T$$

$$K_p = \begin{bmatrix} K_{pm1} & K_{p\delta 1} & K_{pm2} & K_{p\delta 2} \end{bmatrix}^T$$

$$K_q = \begin{bmatrix} K_{qm1} & K_{q\delta 1} & K_{qm2} & K_{q\delta 2} \end{bmatrix}^T$$

$$K_v = \begin{bmatrix} K_{vm1} & K_{v\delta 1} & K_{vm2} & K_{v\delta 2} \end{bmatrix}^T$$

This model has 28 constants, presented below and, are functions of the system parameters and initial operating condition stated below.The system is incorporated with IPFC. Load flow analysis is performed to obtain the operating point which is given as follows:

$P_e = 0.900$, Q = 0.1958 $V_s = 1.02$

$V_b = 1$ $V_{pq1} = 0.3795$ $V_{do} = 0.4311$

$V_{qo} = 0.9244$ $I_{do} = 0.5469$ $I_{qo} = 0.7185$

$\delta_o = 7.6056^\circ$ $\delta_{1o} = 71.5651^o$ $\delta_{2o} = 7.725^o$

The system is linearized about this operating point. The K-constants for the system installed with IPFC, are computed as follows:

$K_1 = 2.0552$ $K_2 = 0.0413$

$K_3 = 0.7333$ $K_4 = 0.000001$

$K_5 = 0.0185$ $K_6 = 0.6001$

$K_7 = -0.0885$ $K_8 = -0.1088$

$K_9 = 7.6663 \times 10^{-4}$ $K_{pv} = 0.0672$

$K_{qv} = -0.0087$ $K_{vv} = -0.0116$

$K_{pm1} = 0.0552$ $K_{pm2} = 0.2530$

$K_{p\delta 1} = 0.0376$ $K_{p\delta 2} = -0.0045$

$K_{qm1} = -0.0326$ $K_{q\delta 1} = 0.0010$

$K_{qm2} = 0.0056$ $K_{q\delta 2} = 0.0033$

$K_{vm1} = -0.0360$ $K_{v\delta 1} = -0.0029$

$K_{vm2} = -0.0038$ $K_{v\delta 2} = -0.0021$

Journal of Theoretical and Applied Information Technology
20th January 2013. Vol. 47 No.2

ISSN: 1992-8645 www.jatit.org E-ISSN: 1817-3195

$K_{cm1} = 7.6663\times10^{-4}$ $K_{c\delta1} = 0.0672$
$K_{cm2} = -0.0087$ $K_{c\delta2} = -0.0116$

4. DESIGN OF IPFC DAMPING CONTROLLERS

To improve the damping of low frequency oscillations the damping controllers are provided to produce the additional damping torque. The speed deviation $\Delta\omega$ is considered as the input to the damping controllers which reflects the swings on the machines and lines of interest. As such, the output of the controller is in phase with the speed deviation.

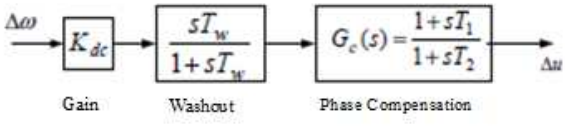

Fig. 3 Structure of IPFC based damping controller

The structure of IPFC based damping controller is shown in Fig.3. It consists of gain, signal washout and phase compensation blocks. The optimum parameters of the damping controller are obtained using the phase compensation technique [4]. The design is presented as below. The time constants of the phase compensator are chosen such that the phase angle of the system is fully compensated. For the nominal operating condition, the magnitude and phase angle of transfer function, $\Delta P_e/\Delta U$, will be computed for $s = j\omega_n$. The gain setting of the damping controller is chosen to achieve the required damping ratio of 0.1. As observed from (24) there are four choices of input signals ($m_1, \delta_1, m_2 \text{ and } \delta_2$) of the IPFC to modulate. The signal which can achieve effective damping control at minimum control cost will be the most efficient. This selection is made at open loop condition before installation of damping controller. The concept of controllability index is used to select the most suitable IPFC control parameter from the damping controller for modulation [5].

(1). Compute the natural frequency of oscillation ω_n from the mechanical loop as

$$\omega_n = \sqrt{K_1\omega_o / M}$$

(2). Let γ be the angle of the transfer function $G_s(s) = \frac{\Delta P_e}{\Delta u}$,(phase lag of between Δu and ΔP_e , where $\Delta u = \left[\Delta m_1, \Delta\delta_1, \Delta m_2 \text{ and } \Delta\delta_2\right]$ as shown in Fig.4.5, at $s = j\omega_n$.

(3). The controller designed is made up of washout filter and lead-lag block, with the following transfer function:

$$G_s(s) = K\frac{sT_w}{1+sT_w}\cdot\frac{1+sT_1}{1+sT_2}$$

T_w is the washout filter time constant and its value can be taken as a number between 1 and 20 *sec*. Assume for the lead-lag network, $T_1 = aT_2$, where a = (1+ sinγ) /(1− sinγ)

and $T_2 = 1/\left(\omega_n\sqrt{a}\right)$. The required gain setting for the desired ratio ξ is obtained as,

$K = \frac{2\xi\omega_n M}{|G_c(s)||G_s(s)|}$, where $|G_c(s)|$ and $|G_s(s)|$ are evaluated at $s = j\omega_n$.

The eigen values corresponding to oscillatory modes of the system are computed as given in table 1. From the table 1, we observe that the system consists of both local modes and inter area modes. The inter area modes are sufficiently damped, whereas, the local modes are lightly damped.

Table 1: Eigen Values Of The System

Eigen values	Damping ratio of Oscillatory modes	Natural frequency of Oscillations(Hz)
$-0.0032 \pm 9.8410\,j$	0.0003	1.5662
$-10.0698 \pm 4.5122\,j$	0.9126	0.7181
-0.0000291	1.000	0

For the nominal operating point, the natural frequency of oscillation ω_n is equal to 9.8410j rad/sec. This mode is responsible for the low frequency oscillation of around 1.5 Hz with very less damping of 0.0003. The damping controllers are designed to provide the additional damping. The parameters of the controllers are computed assuming a damping ratio (ξ) of 0.1. The gain and

Journal of Theoretical and Applied Information Technology
20th January 2013. Vol. 47 No.2

ISSN: 1992-8645 www.jatit.org E-ISSN: 1817-3195

phase angle of $G_c(s)$ for the various inputs are computed and given in table 2.

Table 2: Magnitude And Phase Angle Of The Transfer Function

$G_c(s)$	$\lvert G_c(s)\rvert$	$\angle G_c(s)$
$\Delta P_e/\Delta m_1$	0.055447	-1.5426^o
$\Delta P_e/\Delta \delta_1$	0.037634	-0.89511^o
$\Delta P_e/\Delta m_2$	0.25303	-0.042285^o
$\Delta P_e/\Delta \delta_2$	0.0044907	-179.98^o

It can be seen that the phase angle of the system for the control parameter $\Delta\delta_2$ is near to -180° therefore the system becomes unstable when the controller ($\Delta\delta_2$) is used. This controller is not considered in further investigations. Table 3 shows parameters of the remaining three alternative damping controllers computed at the nominal operating point.

Table 3: Parameters Of The Ipfc Damping Controllers

Damping controller	K	T_1
Damping controller Δm_1	276.44	0.10439
Damping controller $\Delta\delta_1$	411.91	0.10439
Damping controller Δm_2	62.183	0.10169

In the next chapter response of Δω with the three alternative damping controllers is simulated. The response of Δω is obtained with a step perturbation of ΔP_m = 0.01. Simulation results shows that the responses are identical which indicates that any of the IPFC damping controllers, provide satisfactory performance at the nominal operating point.

However, in order to select the most effective IPFC control signal for damping, the controllability index is computed. The index is computed for the electromechanical mode (9.8410jrad/sec) to be damped taking into account all the control signals one at a time. Table 4 gives the computed values of the indices.

Table 4: Controllability Indices With Different Ipfc Controllable Parameters

IPFC control parameter	Controllability Index
Δm_1	0.17974
Δm_2	0.8202
$\Delta\delta_1$	0.12194
$\Delta\delta_2$	0.014551

Table 4 reveals that the controllability index corresponding to IPFC control parameter Δm_2 , is highest and that of $\Delta\delta_2$, is insignificant compared to the other control parameters. Hence, $\Delta u = \Delta m_2$ is the best selection for the design of the IPFC damping controller since the minimum control cost (the lowest gain) is needed to provide now on, the damping controllers based on Δm_2 shall be denoted as damping controller Δm_2 . In the next chapter the dynamic response of the system with and without the damping controller Δm_2 is studied.

The dynamic performance of the system is further examined considering a case in which two Δm_1 , Δm_2 damping controllers operate simultaneously **(dual controller).**

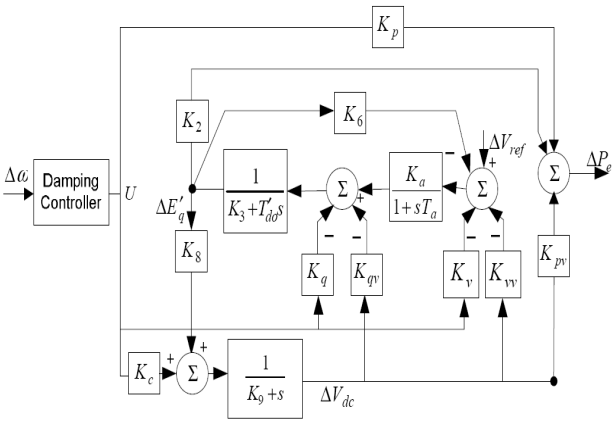

Fig. 4 Transfer function of the system relating component of electrical power ΔP_e produced by damping controller Δu

Journal of Theoretical and Applied Information Technology
20th January 2013. Vol. 47 No.2

ISSN: 1992-8645 www.jatit.org E-ISSN: 1817-3195

Table 5: Phillips-Heffren Model Constants For System Without Ipfc

i	K_i
1	3.2944
2	0.8533
3	1.2308
4	0.0640
5	-0.0150
6	0.9220

5. DIGITAL SIMULATION

In order to understand the effect of IPFC on damping low frequency oscillations, digital simulations using Matlab Simulink toolbox is done in two cases, with and without IPFC.The block diagram of fig 27 is used in small signal stability investigations of the power system. The MATLAB Simulink toolbox is used to study the system performance under different damping controllers. Following figures shows the results of SMIB with different damping controllers. The rotor speed deviations and rotor angle deviations, respectively for different damping controllers are studied. The damping controllers are designed by two methods.

1) The speed deviation (Δω) is used as input signal for design of damping controllers using phase compensation technique [4].
2) The electrical power is taken as input for the design of PI-Damping controllers [3,8].

6. SIMULATION RESULTS

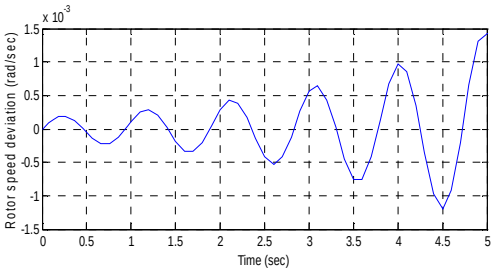

Fig 5. Rotor speed deviation for ΔP_m = 0.01, without IPFC

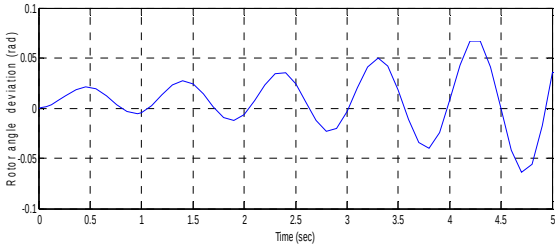

Fig 6. Rotor angle deviation for ΔP_m = 0.01, without IPFC

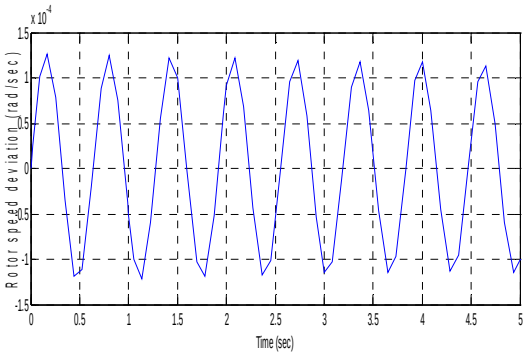

Fig 7 Rotor Speed deviation for ΔP_m = 0.01, without (Δm_2)IPFC controller

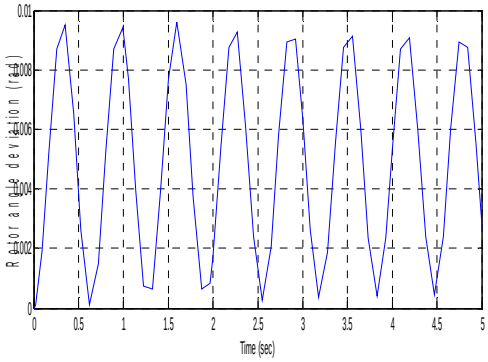

Fig 8. Rotor angle deviation for ΔP_m = 0.01, without (Δm_2) IPFC controller

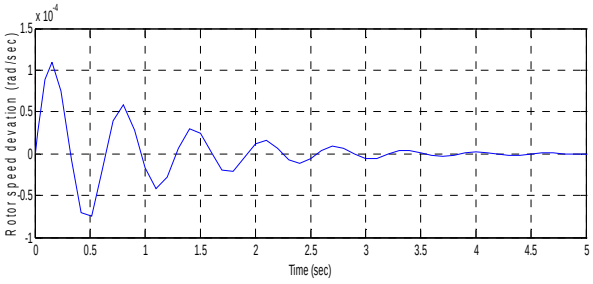

Fig 9. Rotor speed deviation for ΔP_m = 0.01, with (Δm_2) type damping controller

Journal of Theoretical and Applied Information Technology
20th January 2013. Vol. 47 No.2

ISSN: 1992-8645 www.jatit.org E-ISSN: 1817-3195

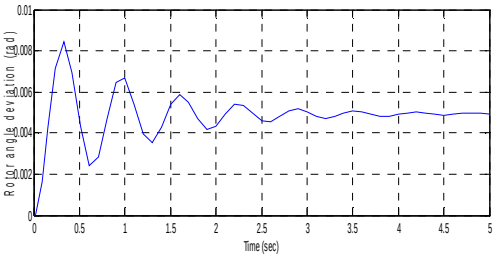

Fig 10 Rotor angle deviation for ΔP_m = 0.01, with (Δm_2) type damping controller

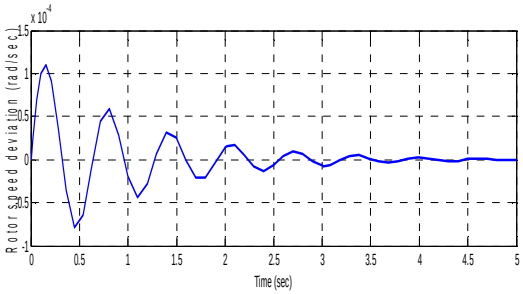

Fig 11 Rotor speed deviation for ΔP_m = 0.01, with (Δm_1) type damping controller

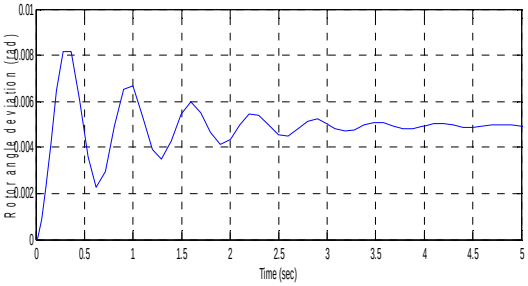

Fig 12 Rotor angle deviation for ΔP_m = 0.01, with (Δm_1) type damping controller

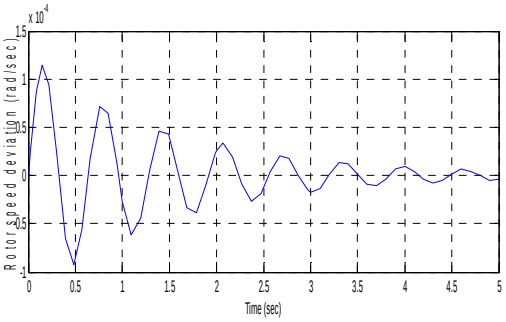

Fig 13. Rotor speed deviation for ΔP_m = 0.01, with ($\Delta \delta_1$) type damping controller

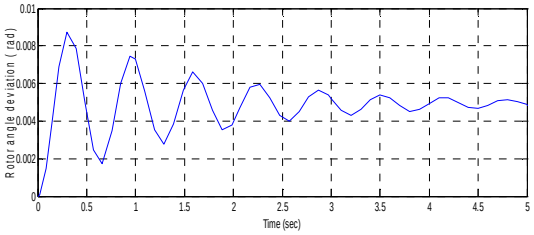

Fig 14. Rotor angle deviation for ΔP_m = 0.01, with ($\Delta \delta_1$) type damping controller

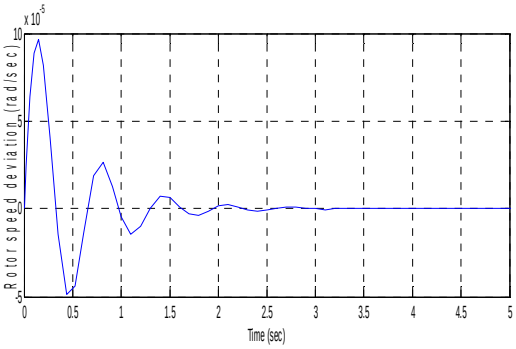

Fig 15. Rotor speed deviation for ΔP_m = 0.01, with dual damping controller

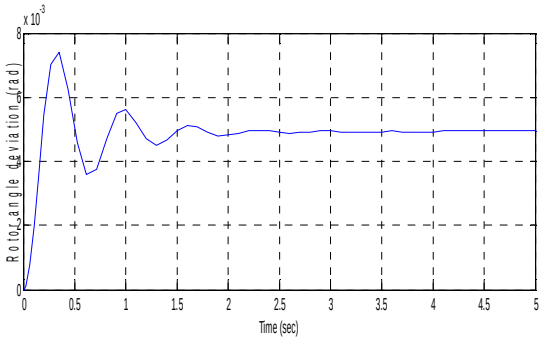

Fig 16. Rotor angle deviation for ΔP_m = 0.01, with dual damping controller

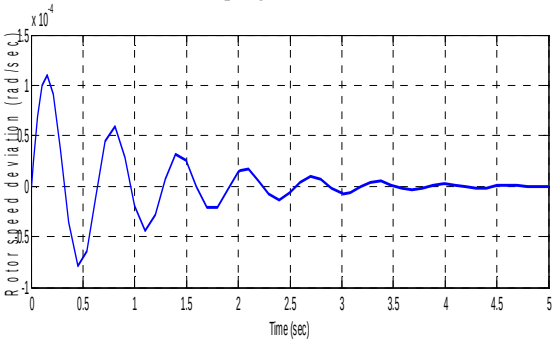

Fig 17. Rotor speed deviation at P_e = 0.2, with (Δm_2) type damping controller

Journal of Theoretical and Applied Information Technology
20th January 2013. Vol. 47 No.2

ISSN: 1992-8645 www.jatit.org E-ISSN: 1817-3195

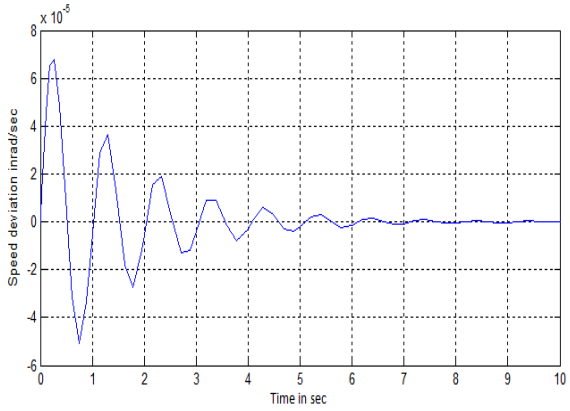

Fig 18. Rotor speed deviation at P_e = 1, with (Δm_2) type damping controller

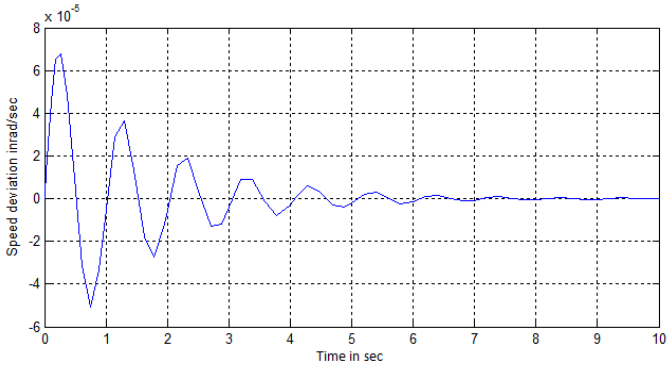

Fig 21 Rotor Speed deviation for ΔP_m = 0.01, with (Δm_2) PI type damping controller

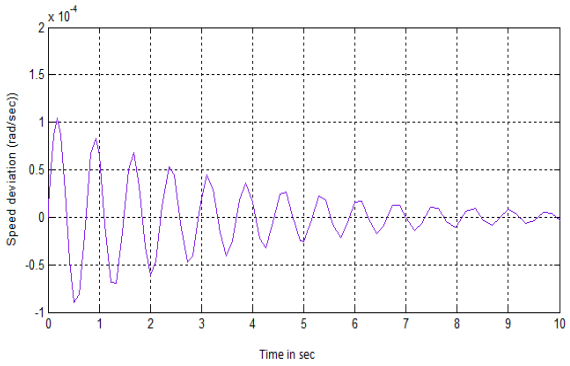

Fig 19 Rotor speed deviation for ΔP_m = 0.01, with (Δm_1) type PI-damping controller

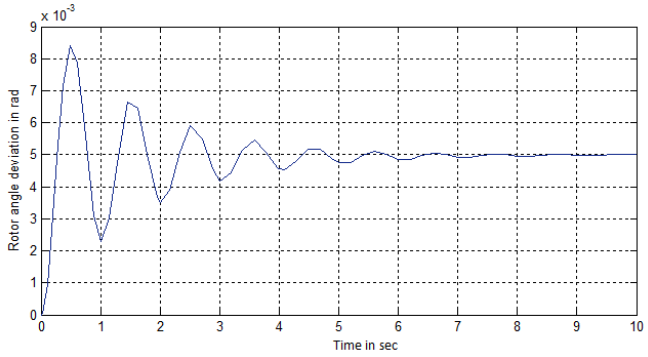

Fig 22. Rotor angle deviation for ΔP_m = 0.01, with (Δm_2) PI type damping controller

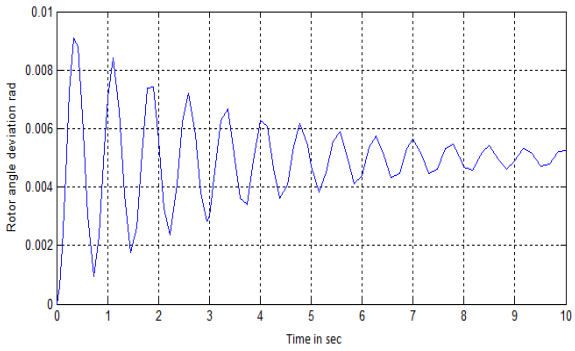

Fig 20. Rotor angle deviation for ΔP_m = 0.01, with (Δm_1) type PI- damping controller

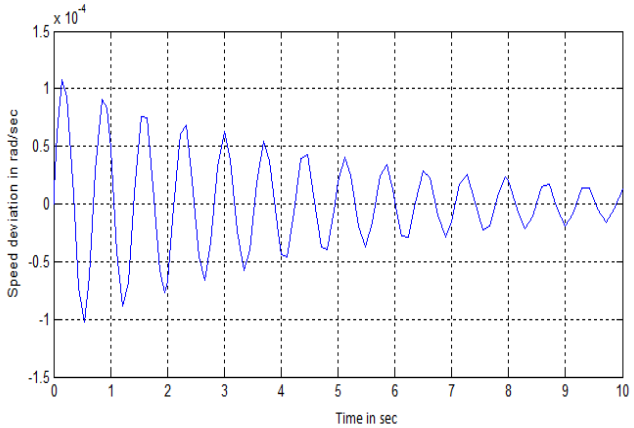

Fig 23 Rotor speed deviation for ΔP_m = 0.01, with($\Delta \delta_1$) PI type damping controller

Journal of Theoretical and Applied Information Technology
20th January 2013. Vol. 47 No.2

ISSN: 1992-8645 www.jatit.org E-ISSN: 1817-3195

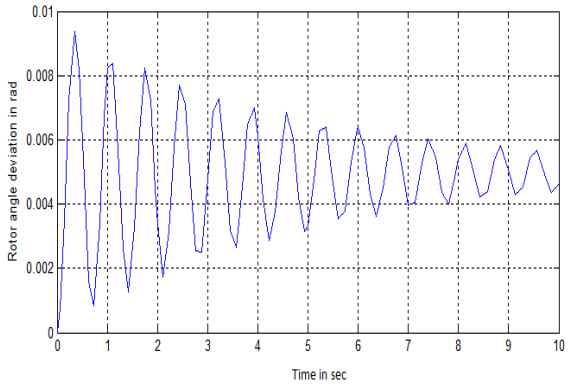

Fig 24 Rotor angle deviation for ΔP_m *= 0.01, with(* $\Delta\delta_1$ *) PI type damping controller*

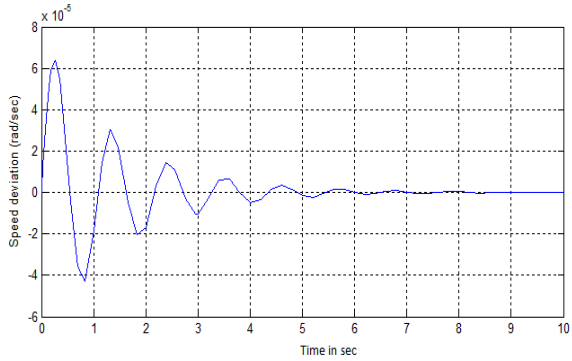

Fig 25 Rotor speed deviation for ΔP_m *= 0.01, with PI-dual damping controller*

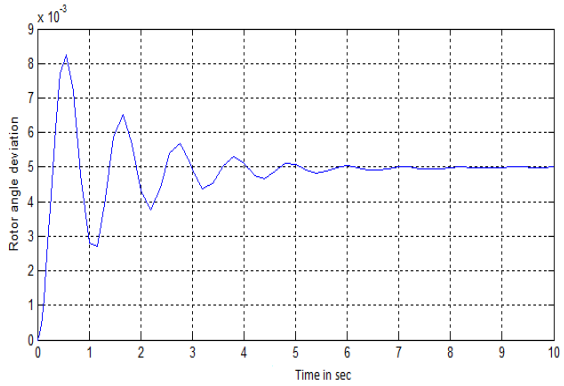

Fig 26 Rotor angle deviation for ΔP_m *= 0.01, with PI-dual damping controller*

7. CONCLUSIONS

The IPFC based damping controller is designed for two different cases. The output of the power system without IPFC, with IPFC are obtained and compared.

IPFC as a multitask controller, has an effective role in damping low frequency oscillations. In this thesis, this function of IPFC has been investigated and numerical results emphasized its significant effect. In fact, even there is not any damping coefficient in power systems, IPFC can damp low frequency oscillations. These effects are decreasing the amplitude and frequency of power system oscillations. Moreover it damps oscillations faster in comparison when there is not IPFC in the system. The controllability index corresponding to IPFC control parameter Δm_2 , is highest and that of $\Delta\delta_2$, is insignificant compared to the other control parameters. Hence, $\Delta u = \Delta m_2$ is the best selection for the design of the IPFC damping controller since the minimum control cost (the lowest gain) is needed to provide , the damping controllers based on Δm_2 .

Dynamic simulations results have emphasized that the damping controller which modulates the control signal Δm_2 provides satisfactory dynamic Performance under wide variations in loading condition and system parameters.

The response of the SMIB installed with IPFC based Dual converter is improved when compared to without IPFC and individual (m_1 , δ_1 ,and m_2) type damping controllers. Response of SMIB with IPFC for step perturbation in ΔP_m = 0.01 ,and ΔV_{ref} = 0.01 is good with Dual controller.

The settling time for PI- damping controller is more as compared to Phase-compensation based damping controllers. Phase-compensation based damping controllers damps oscillations faster in comparison with PI-controllers.

ISSN: 1992-8645 www.jatit.org E-ISSN: 1817-3195

Table 6: Comparison of Settling Time for Two cases

IPFC damping controller	PI Controller	Phase Compensation
m_1 -type controller	10 sec	4.5 sec
δ_1 -type controller	10 sec	5 sec
m_2 -type controller	9 sec	4 sec
Dual converter	8 sec	3 sec

APPENDIX

The system data and initial operating conditions of the system are as follows:

Generator:
M = 2H = 8.0 MJ/MVA
D = 0; *Tdo* = 5.044s; X_d =1.0pu; X'_d = 0.3pu;
X_q = 0.6pu ; P_e = 0.900; Q = 0.1958; V_s = 1.02;
$V_b = 1$

Excitation system: K_A = 50; T_A = 0.05s
Converter transformers: X_t = 0.l pu
Converter parameters: m_1 = 0.15; m_2 =0.10;
Transmission line transformers:
X_L = 0.5 pu; X_s =0.15 pu
DC link parameters: V_{dc} = 2.0 pu; C = 1 pu

REFERENCES

[1] Yao-nan Yu, "ELECTRIC POWER SYSTEM DYNAMICS", New York, Academic Press, Inc. , 1983
[2] Guygyi & etal " THE INTERLINE POWER FLOW CONTROLLER CONCEPT: A NEW APPROACH TO POWER FLOW MANAGEMENT IN TRANSMISSION SYSTEMS", IEEE Transactions on Power Delivery, Vol. 14, No. 3, July 1999.
[3] H.F.Hang, "DESIGN OF SSSC DAMPING CONTROLLER TO IMPROVE POWER SYSTEM OSCILLATION STABILITY", 19991EEE.
[4] N.Tambey and M.L.Kothari, "DAMPING OF POWER SYSTEM OSCILLATION WITH UNIFIED POWER FLOW CONTROLLER", IEE Proc.-Gener. Transm. Distrib. Vol.150, No.2, March 2003.
[5] "FLEXIBLE AC TRANSMISSION SYSTEMS (FACTS)", IEE Press, London 1999.
[6] K. V. Patil, J. Senthil, J. Jiang and R. M. Mathur, "Application of STATCOM for Damping Torsional Oscillations in Series Compensated AC Systems," IEEE Transactions on Energy Conversion, vol. 13, No. 3, September 1998, pp. 237-243.
[7] H.F.Wang and F.J.Swift, "A Unified Model for the Analysis of FACTS Devices in Damping Power System Oscillations Part I: Single-Machine Infinite-bus Power
System," IEEE Transactions on Power Delivery, vol. 12, No. 2, April 1997, pp. 941-946.
[8] L. Fan and A. Feliachi, "Robust TCSC Control Design for Damping Inter-Area Oscillations," Proceedings of 2001 IEEE PES Summer Meeting, Vancouver, British Columbia, Canada, July 15-19, 2001.

ISSN: 1992-8645 www.jatit.org E-ISSN: 1817-3195

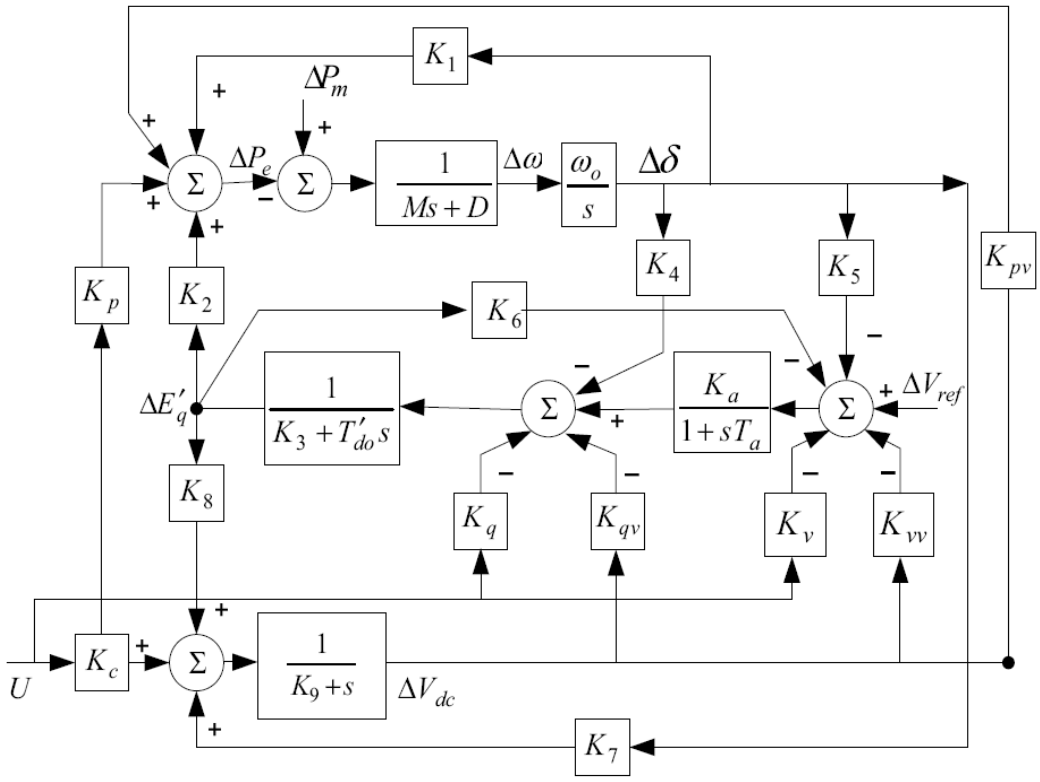

Fig 27. Phillips-Heffron Model (Linearised Model) Of A Single-Machine Infinite-Bus (SMIB) System With IPFC